Author's Accepted Manuscript

Single-molecule porphyrin-metal ion interaction and sensing application

Keke Wei, Fujun Yao, Xiao-feng Kang

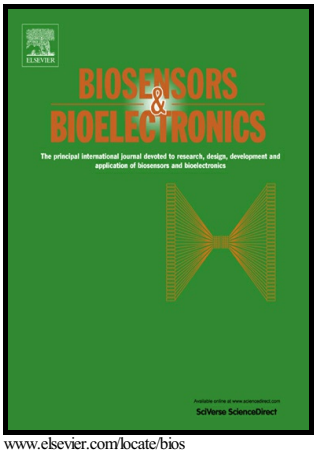

www.elsevier.com/locate/bios

PII: S0956-5663(18)30167-2
DOI: https://doi.org/10.1016/j.bios.2018.03.002
Reference: BIOS10328

To appear in: *Biosensors and Bioelectronic*

Received date: 5 January 2018
Revised date: 19 February 2018
Accepted date: 1 March 2018

Cite this article as: Keke Wei, Fujun Yao and Xiao-feng Kang, Single-molecule porphyrin-metal ion interaction and sensing application, *Biosensors and Bioelectronic,* https://doi.org/10.1016/j.bios.2018.03.002

This is a PDF file of an unedited manuscript that has been accepted for publication. As a service to our customers we are providing this early version of the manuscript. The manuscript will undergo copyediting, typesetting, and review of the resulting galley proof before it is published in its final citable form. Please note that during the production process errors may be discovered which could affect the content, and all legal disclaimers that apply to the journal pertain.

ACCEPTED MANUSCRIPT

Single-molecule porphyrin-metal ion interaction and sensing application

Keke Wei[1], Fujun Yao[1], Xiao-feng Kang[*]

Key Laboratory of Synthetic and Natural Functional Molecular Chemistry, College of Chemistry & Materials Science, Northwest University, Xi'an 710069, P. R. China

[*]Corresponding author. Tel.: +86-029-88302604; fax: +86-029-88302604.

kangxf@nwu.edu.cn

Accepted manuscript

Abstract

It remains a significant challenge to study the interactions between metal ions and porphyrin molecules at single ion level. Here, we constructed a nanopore-based sensing for label-free and real-time analysis of the interaction between Cu^{2+} and 5,10,15,20-tetrakis(4-sulfonatophenyl)-porphyrin (TPPS). The results demonstrate that emerging electronic signatures of the Cu^{2+}-TPPS complex that is completely different form the original free TPPS were observed in the α-hemolysin (α-HL) nanopore. Based on the distinctive electronic signal patterns between TPPS and Cu^{2+}-TPPS complex, the unique nanopore sensor can achieve a highly sensitive detection of Cu^{2+} in aqueous media. The frequency of signature events showed a

[1] These authors contributed equally to this work.

ACCEPTED MANUSCRIPT

linear response toward the concentration of Cu^{2+} in the range of 0.03 μM – 1.0 μM, with a detection limit of 16 nM (S/N = 3). The sensing system also exhibited high selectivity against other metal ions, and the feasibility of this approach for practical applications was demonstrated with the determination of Cu^{2+} in running water.

Keywords: α-hemolysin nanopore; single-molecule detection; TPPS; copper ion; biosensor

1. Introduction

Sensing of metal ions in aqueous solutions is of great importance in terms of their widespread distribution in environmental systems and biological processes. Among all the metal ions, copper is an essential trace metal that plays fundamental roles in many physiological processes by serving as a cofactor for numerous proteins and enzymes (Domaille et al., 2008). However, excess copper intake can cause damage to liver, kidney and nervous system (Boal and Rosenzweig 2009). Consequently, the development of facile, sensitive and reliable methods for identification and quantification of copper ions is in high demand.

Conventional techniques for copper ions detection include atomic absorption or emission spectroscopy (AAS/AES) (Kumar et al., 2011; Lima et al., 2012), and inductively coupled plasma mass spectrometry (ICP-MS) (Dai et al., 2012). Although these techniques can detect metal ions sensitively and accurately, and are considered as standard methods, they usually require sophisticated instruments, tedious sample

Accepted manuscript

preparation procedures and trained personnel. All of these shortcomings limit their wide applications in routine copper ion detection. Alternatively, colorimetric and fluorescent chemosensors based on small organic molecules have been intensively developed for the detection of Cu^{2+} ions. Unfortunately, these chemosensors typically suffer from low selectivity and poor water solubility, making it difficult to monitor Cu^{2+} ions in practical applications. Recently, some highly sensitive methods for Cu^{2+} detection have been proposed by employing catalytic DNAzyme (He et al., 2014; Xu et al., 2015; Yin et al., 2009), for examples, electrochemistry (Yang et al., 2016), colorimetry (Sadollahkhani et al., 2014; Yuan et al., 2014; Z et al., 2014), quantum dots (Dong et al., 2012) and molecular beacon (Brunner and Kraemer 2004) based on transforming the target-specific activity of DNAzymes into detectable optical or electric signals. These DNAzymes-based sensors have good specificity and sensitivity, but most of them need labeling tags, which not only increase the cost and complication of the sensing system, but also decrease its biocompatibility. Accordingly, it is still a great challenge to develop a simple and label-free method for Cu^{2+} ions detection with high sensitivity. In this work, we develop a new method for the determination of Cu^{2+} ions by integrating a water-soluble small organic molecules-based probe with the α-HL nanopore.

Nanopore is an emerging single-molecule analytical technology. Its inherent merits such as label-free, ultrasensitivity, high signal-to-noise ratio and single-molecule resolution, make it a powerful single-molecule identifier and detector for DNAs (Venkatesan and Bashir 2011), RNAs (Zhang et al., 2015), peptides

Accepted manuscript

(Asandei et al., 2013; Roozbahani et al., 2017; Yusko et al., 2012), proteins (Rotem et al., 2012), biomarkers (Tian et al., 2017) as well as small molecules (Boersma et al., 2012). With regard to metal ions detection, nanopore-based technologies have been successfully used to detect a variety of metal ions including Cu^{2+} (Wang et al., 2017), Co^{2+}, Cd^{2+}, Hg^{2+} (Wen et al., 2011), Pb^{2+}, Ba^{2+} (Yang et al., 2013) and UO_2^{2+} (Roozbahani et al., 2017). Different sensing strategies including noncovalent or covalent binding sites embedded within the pores, thymine-thymine mismatches in DNA (Wen et al., 2011), G-quadruplex DNA (Yang et al., 2013), DNAzymes (Yin et al., 2014) and peptides (Roozbahani et al., 2017) have been reported with high sensitivity and selectivity. However, so far few studies have dealt with the detection of metal ions by combining small organic molecule-based probes and nanopore sensor.

In this work, we employed TPPS as a recognition probe for highly selective Cu^{2+} detection based on α-HL nanopore sensor. Distinctive electronic signatures of Cu^{2+}-TPPS complexes were generated in the nanopore, which were different form the original TPPS. By analyzing these new signatures, quantitative detection of Cu^{2+} ions could be achieved. In comparison with previously reported Cu^{2+}-specific detection methods such as electrochemistry and fluorescence, the present nanopore sensor provides a simple, label-free and amplification-free technique, which can be used to study the interactions between TPPS and Cu^{2+} at single ion level. The whole detection process does not need long time and tedious steps, making the sensing system simple and cost-effective. In addition, the proposed method can also be successfully applied to the determination of Cu^{2+} ions in running water.

Accepted manuscript

ACCEPTED MANUSCRIPT

2. Experimental section

2.1 Materials and regents

5,10,15,20-tetrakis(4-sulfonatophenyl)-porphyrin were purchased from J & K chemical. Tetramethylammonium chloride (TMA-Cl), $CuCl_2$ were purchased from Sigma-Aldrich. 2-Diphytanoylphosphatidylcholine (DPhPC) lipid was obtained from Avanti Polar Lipids (USA). The thickness of Teflon film (Good fellow) was 25 μm. The wild-type (WT) α-HL monomers were expressed in Escherichia coli BL-21 (DE3) pLysS and purified by size exclusion chromatography. The assembly and purification of heptametrical protein pores were carried out as reported previously (Cheley et al., 1999).

2.2 Single-Channel Recording

A bilayer of DPhPC was formed over a 120-150 μm orifice in diameter in a Teflon septum that divided a planar bilayer chamber into cis and trans compartments. The formation of bilayer was achieved using the Montal-Mueller method (Montal and Mueller 1972). The solutions in the compartments contained 1 M TMA-Cl, which was buffered with 10 mM PB at pH 7.0 and 8.0, and 10 mM NaAc/HAc at pH 5.2 and 6.0, respectively. α-HL proteins and TPPS were added to the cis compartment, which was connected to a "grounded". The final concentration of the α-HL proteins used for the single-channel insertion was 0.05-0.2 ng/mL. Current were recorded with a patch-clamp amplifer (Axopatch 200B, Molecular Devices, Sunnyvale, CA), filtered with a built-in four-pole Bessel filler at 5 kHz, sampled at 20 kHz by a computer

Accepted manuscript

equipped with a Digidata 1440A A/D converter (Molecular Devices).

2.3 Data Analysis

Single-channel event amplitude and duration were analyzed using Clampfit 10.5 (Molecular Devices) and origin 9.0 software (Microcal, Northampton, MA). Mean dwell time values (τ_{off}) and mean interevent interval values (τ_{on}) were obtained from the dwell histograms, and the interevent histograms were fitted to single exponential functions. The standard deviation of open pore current (I_0) was obtained from single channel current baseline histograms by fitting the distributions to Gaussian functions. The values of mean signal amplitude and current blocking rate ($\Delta I/I_0$) were obtained from signal amplitude and I/I_0 histograms by fitting the distributions to Gaussian functions.

3. Results and discussion

3.1. The principle of Cu^{2+} ions detection using TPPS

The porphyrins and its derivatives are a class of heterocyclic macrocyclic compounds, which play important roles in numerous fields such as catalysis, materials and medicine (Ding et al., 2017; R et al., 2017). In these compounds, four pyrroline subunits interconnected by their α carbon atoms through methine bridges (=CH-). The multiple pyrrolic N atoms in the planar tetrapyrrolic macrocyle lead to unique metal ion binding affinity and selectivity (Ding et al., 2017). By taking advantage of the photophysical characteristics such as quite different emission properties of the metallo- and free base porphyrin, various porphyrin-based chemosensors have been

Accepted manuscript

developed for the detection of heavy metal ions (Bill et al., 2015; He et al., 2006; Pariyar et al., 2012; Santos et al., 2013).

The principle of nanopore assay for Cu^{2+} detection is shown in Scheme1. In the absence of Cu^{2+}, the interaction of TPPS with the α-HL protein nanopore only generated short-lived and low amplitude events. In contrast, with the addition of Cu^{2+} to the solution, it can incorporate into the small-size coordination cavity of TPPS, leading to the formation of stable Cu^{2+}-TPPS complexes. The subsequent interaction between Cu^{2+}-TPPS and α-HL pore result in long-lived events with high amplitude. Therefore, based on the different characteristic signatures, Cu^{2+} could readily be determined.

3.2. Detection of Cu^{2+} ions using TPPS

To demonstrate the feasibility of this concept, we first conducted an analysis of TPPS interaction with the *α*-HL pore. Recordings were made in solutions containing 1 M tetramethylammonium chloride (TMA-Cl), buffered with 10 mM NaAc, at pH 5.2. We chose TMA-Cl, instead of KCl, as pore-filled electrolyte because it can improve the stability of the planar lipid bilayer and reduce the noise of single-channel recording (Wang et al., 2015). In a first set of experiments, we investigated the binding of TPPS to the α-HL pore from the trans side. Since TPPS is a tetravalent anion, negative potential was applied on the membrane so TPPS can be driven electrophoretically into the β-barrel of α-HL pore. After adding 5 μM TPPS to the trans chamber, no current blocking signal was observed at – 140 mV (Fig. 1A). This might be caused by that the diameter of the TPPS molecule (~2 nm) is comparable to

Accepted manuscript

the diameter of the β-barrel (~2 nm), thus TPPS cannot enter into the pore and causes ionic current modulation. Then, when TPPS was added to the cis chamber, characteristic current blocking signals were generated at positive potential of + 140 mV, which resulted from the binding of TPPS with the inner wall of the pore. Typical ionic current traces are shown in Fig. 1B and 1D. The binding events were characterized by the dwell time (τ_{off}) and the normalized blockage current ($\Delta I/I_0$; ΔI represents magnitude of current drop, I_0 is the open pore current). Fig. 1E shows a scatter plot of the $\Delta I/I_0$ versus dwell time of a total of 929 binding events. Fitting the $\Delta I/I_0$ and dwell time histograms to a Gauss function and a single exponential decay function (Fig. 1F and 1G), respectively, yielded mean values of $\Delta I/I_0$ = 0.38 ± 0.04 and τ_{off} = 2.42 ± 0.17 ms (n = 5). Since the diameter of the TPPS molecule is larger than the constriction of α-HL pore (~1.5 nm), it cannot translocate the pore to the trans chamber. Therefore, the current blocks may result from trapped TPPS molecule in the vestibule and then exit the pore from the cis entrance without translocation. The voltage dependence experiments further supported the molecular mechanism. The dwell time of TPPS was prolonged by a factor of 4.73 from 0.71 ms to 3.36 ms as the voltage increased from + 100 mV to + 160 mV (Fig. S1).

Subsequently, when Cu^{2+} is being added in the cis side under identical condition, new events with significantly different signatures were observed (Fig. 1C and 1H). Since Cu^{2+} ions themselves could not produce any current blocking in the nanopore (Fig. S2), the new generated signals should be ascribed to Cu^{2+}-TPPS complexes. The data analysis were shown in Fig. 1J and 1K. In the histogram of dwell time and $\Delta I/I_0$,

Accepted manuscript

ACCEPTED MANUSCRIPT

Cu^{2+}-TPPS complex events displayed a higher mean $\Delta I/I_0$ (0.55 ± 0.03) (n = 5) and increased mean dwell time (73.08 ± 2.42 ms) compared to those of free TPPS. In addition, the scatter plot also displayed remarkably different distribution between free TPPS and Cu^{2+}-TPPS complex (Fig. 1I). The reason why the $\Delta I/I_0$ of Cu^{2+}-TPPS complex events was higher than that of uncomplex TPPS events may be due to configuration distortion of the planar porphyrin molecular with the incorporation of Cu^{2+}, thus leading to the occupation of more space. A possible explanation for the increased dwell time of Cu^{2+}-TPPS complexes events is that the binding of Cu^{2+} to TPPS changes the charge distribution of porphyrin molecules, thus resulting in an enhanced interaction between the Cu^{2+}-TPPS complexes and α-HL pore. The discrimination between the free TPPS and Cu^{2+}-TPPS complexes was readily achieved based on the mean dwell time and the normalized blockage current. These long-lived and deep current blockage events were observed only in the presence of Cu^{2+} ions. The formation of Cu^{2+}-TPPS complexes was also confirmed by UV-Vis spectroscopy (Fig. S3).

3.3. pH effect on the sensitivity of the nanopore sensor

The pH values of the electrolyte solution usually show somewhat of an effect on the properties of the protein pore such as ion selectivity, conductance, surface charge and so on (Wang et al., 2014). It has been well documented that the entry and residence of analytes in nanopore can be controlled by modulating the pH (Gu and Bayley 2000). Therefore, at appropriate pH condition, the capture rate of analytes can be enhanced and the transport rate can be slow down, which will improve the

Accepted manuscript

sensitivity and resolution of the nanopore sensing systems (Merzlyak et al., 2005). To achieve highly sensitive detection of Cu^{2+}, the interactions between TPPS and the α-HL pore in the presence of Cu^{2+} were carried out at different pH values of 5.2, 6.0, 7.0 and 8.0. Our results demonstrated that the entrance frequency and the mean dwell time of Cu^{2+}-TPPS signature events decreased as the pH increased. For example, when the pH changed from 5.2 to 8.0, the signature events frequency decreased from 3.30 ± 0.14 s^{-1} to 0.19 ± 0.20 s^{-1}, and the mean dwell time decreased from 73.08 ± 5.76 ms to 41.6 ± 4.04 ms. Among the four pH values, Cu^{2+}-TPPS complexes showed the largest entrance frequency and the mean dwell time at pH 5.2, with values of 3.30 ± 0.14 s^{-1} and 73.08 ± 5.76 ms (Fig. 2B and 2C). When the pH value is less than 5, the protonation of porphyrin macrocycle (p*K*a ≈ 4.9) is the competing reaction with respect to the coordination of metal ion (Nam et al., 2015). Therefore, the electrolyte buffer solution of pH 5.2 was used in the remaining experiments. In addition, the pH effect on the event frequency and the mean dwell time for free TPPS showed a same trend as that of Cu^{2+}-TPPS complexes (Fig. 2D and 2E).

The pH effect on the detection of Cu^{2+} may be attributed to combined action of electrophoresis (EP) and electroosmosis (EO), which dominated the transport of charged molecules through the nanopore (Gu et al., 2003). As depicted in Fig. 2F, the net charge of the *α*-HL inner surface is positive at pH 5.2, which contributes to an enhanced anionic selectivity of the protein nanopore and electroosmotic flow (EOF) of the fluid. For a positive voltage, the EOF is directed from the cis to the trans side of the α-HL pore. As Cu^{2+}-TPPS complexes are negative charge molecule, EOF and EP

Accepted manuscript

are parallel and therefore enhance the entry of Cu^{2+}-TPPS complexes in the pore. For higher pH 7.0, the α-HL nanopore became weak anionic selectively, so the magnitude of EOF is less significant than that at pH 5.2. Hence the enhancement ability for entry in the pore was weakened. In contrast, the α-HL pore became weak cation selectivity when the pH reached 8.0 (Fig. 2G). Therefore, EOF is directed form the trans to the cis side, which is opposed to the EP movement (antiparallel) and consequently suppress the entry of Cu^{2+}-TPPS complexes in the pore. The pH effect on the dwell time can be also explained by the EOF and EP interpretation. For positive voltage, EOF helps the association of Cu^{2+}-TPPS complexes with the α-HL pore with different degrees for pH 5.2, 6.0 and 7.0. For pH 8.0, EOF resists the association to some extent, and the mean dwell time is a little smaller than that at pH 7.0. Our interpretations are in agreement with previous studies regarding peptide and protein interactions with nanopore at various pH (Firnkes et al., 2010).

3.4 Effect of voltage and TPPS concentration on Cu^{2+} detection

It is well documented that the voltage has a profound effect on the sensitivity of nanopore-based sensing system (Gu et al., 2001). To identify the optimum conditions needed to achieve the maximum nanopore resolution for detection of Cu^{2+}, we further investigated the interactions of TPPS with α-HL nanopore in absence or presence of Cu^{2+} at different voltages ranging from + 100 mV to +160 mV. Our experimental results (Fig. 3B) showed that, in the absence of Cu^{2+}, the frequency of the TPPS events increase as the voltage changing from + 100 mV to + 160 mV. After addition of Cu^{2+} to the TPPS solution, the frequency of characteristic signatures (Cu^{2+}-TPPS

Accepted manuscript

complexes events) (f_{sig}) increased significantly with an increase in the voltage. As shown in Fig. 3A, the +100 mV transmembrane voltage gave the lowest f_{sig} at 0.88 ± 0.12 s^{-1}. f_{sig} increased by a factor of 3.75 to 3.3 ± 0.14 s^{-1} when the applied voltage increased from + 100 mV to + 140 mV. As expected, the applied voltage of + 160 mV achieved the highest f_{sig} at 4.15 ± 0.17 s^{-1} (Fig. 3A). Although the f_{sig} at + 140 mV was slightly lower than that of + 160 mV, + 140 mV was chosen as the optimum applied voltage, and the voltage was employed in the remaining experiments. This is because that the lipid bilayer at + 160 mV was not as stable as that at +140 mV, meanwhile, the spontaneous gating events generated in the α-HL nanopore at +160 mV in TMA-Cl electrolyte would bring interference to Cu^{2+}-TPPS signature events (Fig. S4).

In addition, we also examined the effect of the TPPS concentration on the nanopore sensor sensitivity. We found that the frequency of free TPPS events was linearly proportional to the TPPS concentration, indicating that the concentration of TPPS would not affect the sensitivity of the nanopore sensor. A concentration of 5 μM TPPS was used in the remaining experiments since the single-channel recording experiments demonstrated that TPPS could produce enough events for statistical analysis within a relatively short time (Fig. S5).

3.5 Detection sensitivity and selectivity for Cu^{2+}

To evaluate the sensitivity of the TPPS-based nanopore sensors, Cu^{2+} ions at various concentrations were examined under the optimum conditions (1 M TMA-Cl and 10 mM NaAc/HAc (pH = 5.2), with transmembrane potential of + 140 mV). As

Accepted manuscript

shown in Fig. 4A and 4B, the frequency of Cu^{2+}-TPPS signature events increased with increased Cu^{2+} concentration. Linear regression analysis showed good linearity between the signature event frequency and Cu^{2+} ion concentrations in the range of 0.03 μM -1.0 μM with a correlation coefficient of 0.995 (Fig. 4B, inset; linear regression equation: $f_{sig} = 1.74[Cu^{2+}] + 0.061$). The limit of detection (LOD) was estimated to be 16 nM at a signal-to-noise ratio of 3 in about 10 min of single-channel recording, which is much lower than the US EPA-defined maximal contamination level for copper (20 μM) in water (Yin et al., 2014). Table S1 summarizes other Cu^{2+} detection methods reported in the literatures. Although the LOD of our nanopore sensor was slightly higher than those of sensitive fluorescent and electrochemical sensor for Cu^{2+}, it is still sensitive enough to monitor the Cu^{2+} in environmental analysis.

Besides sensitivity, the selectivity of the sensing method was also evaluated by using other metal ions in place of copper, including Mg^{2+}, Al^{3+}, Ca^{2+}, Cr^{3+}, Mn^{2+}, Fe^{2+}, Fe^{3+}, Co^{2+}, Ni^{2+}, Zn^{2+}, Ag^{+}, Cd^{2+}, Ba^{2+}, Pd^{2+}, Hg^{2+}, and Pb^{2+} at concentrations of 100 μM. The single-channel recording experiments demonstrated that no new signature events generated in the α-HL nanopore except the free TPPS signals. In addition, our results also revealed that the coexistence of Cu^{2+} and other metal ions did not affect detection by the sensor (Fig. S6). Hence the specificity in the detection of Cu^{2+} is not compromised by complex mixtures of other metal ions, which is very common in real samples analysis. All these results indicated that the other metal ions could not interfere with this Cu^{2+} sensing system. The high selectivity of the

Accepted manuscript

TPPS-based nanopore sensor may be due to the unique interactions between Cu^{2+}-TPPS complexes and the vestibule of α-HL nanopore.

3.6 Detection of Cu^{2+} in running water

The feasibility of this TPPS-based nanopore sensor for real-world applications was demonstrated with the determination of Cu^{2+} in running water. In order to ensure the reliability of the experiment, we employed tap water from our laboratory instead of ultrapure water to prepare 1 M TMA-Cl and 10 mM NaAc/HAc (pH = 5.2) buffer solution (real water samples without any pretreatment). The Cu^{2+} in the real water were finally estimated to be 0.12 μM. Moreover, satisfactory recovery in the range of 95.0 to 101.7% was obtained as shown in table 1, and confirmed that this sensor is a powerful tool for the detection of Cu^{2+} in real samples.

Conclusions

In conclusion, we have developed a biosensor for the determination of sub-nM amount of Cu^{2+} by α-HL nanopore combined with a small molecule probe, TPPS. Compared to conventional sensing approaches, the α-HL nanopore biosensor displays several significant advantages, including simplicity, rapid response, label-free, anti-interference and feasibility for practical applications. This promising sensing platform enables rapid and accurate detection of Cu^{2+} with a low detection limit (16 nM). Experiments of running water demonstrated the present method could be extended to Cu^{2+} detection in real samples. This investigation has also provided a

Accepted manuscript

methodology of designing and constructing nanopore biosensors with excellent selectivity and specificity for determination of biologically and environmentally relevant analytes by using desirable molecular recognition probes.

Acknowledgment

This work was financially supported by the National Science Foundation of China (Grants 20175105, 21375104, and 21327806), the Specialized Research Fund for the Doctoral Program of Higher Education of China (Grant 20126101110015), Natural Science Basic Research Plan in Shaanxi Province of China (Grant 2016JQ2021), Scientific Research Program Funded by Shaanxi Provincial Education Department (Grant 16JK1780) and The Science Foundation of Northwest University (No. 338020018).

Accepted manuscript

References

Asandei, A., Schiopu, I., Iftemi, S., Mereuta, L., Luchian, T., 2013. Langmuir 29, 15634-15642.

Bill, N.L., Trukhina, O., Sessler, J.L., Torres, T., 2015. Chem. Commun. 51, 7781-7794.

Boal, A.K., Rosenzweig, A.C., 2009. Chem. Rev. 109, 4760-4779.

Boersma, A.J., Brain, K.L., Bayley, H., 2012. ACS Nano 6, 5304-5308.

Brunner, J., Kraemer, R., 2004. J. Am. Chem. Soc. 126, 13626-13627.

ACCEPTED MANUSCRIPT

Cheley, S., Braha, O., Lu, X., Conlan, S., Bayley, H., 1999. Protein Sci. 8, 1257-1267.

Ding, Y., Zhu, W.H., Xie, Y., 2017. Chem. Rev. 117, 2203-2256.

Domaille, D.W., Que, E.L., Chang, C.J., 2008. Nat. Chem. Biol. 4, 168-175.

Firnkes, M., Pedone, D., Knezevic, J., Döblinger, M., Rant, U., 2010. Nano Lett. 10, 2162-2167.

Gu, L.Q., Bayley, H., 2000. Biophys. J. 79, 1967-1975.

Gu, L.Q., Cheley, S., Bayley, H., 2001. J. Gen. Physiol. 118, 481-494.

Gu, L.Q., Cheley, S., Bayley, H., 2003. Proc. Natl. Acad. Sci. U.S.A. 100, 15498-15503.

He, C.L., Ren, F.L., Zhang, X.B., Han, Z.X., 2006. Talanta 70, 364-369.

He, Y., Tian, J., Zhang, J., Chen, S., Jiang, Y., Hu, K., Zhao, Y., Zhao, S., 2014. Biosens. Bioelectron. 55, 285-288.

Kumar, B.N., Venkata Ramana, D.K., Harinath, Y., Seshaiah, K., Wang, M.C., 2011. J. Agric. Food Chem. 59, 11352-11358.

Merzlyak, P.G., Capistrano, M.F.P., Valeva, A., Kasianowicz, J. J., Krasilnikov, O.V., 2005. Biophys. J. 89, 3059-3070.

Montal, M., Mueller, P., 1972. Pro. Natl. Acad. Sci. U. S.A. 69, 3561-3566.

Nam, D.T., Ivanova, Y.B., Puhovskaya, S.G., Kruk, M.M., Syrbu, S.A., 2015. RSC Adv. 5, 26125-26131.

Pariyar, A., Bose, S., Chhetri, S.S., Biswas, A.N., Bandyopadhyay, P., 2012. Dalton Trans. 41, 3826-3831.

Paolesse,R., Nardis,S., Monti,D., 2017. Chem. Rev. 117, 2517-2583.

Accepted manuscript

Roozbahani, G.M., Chen, X., Zhang, Y., Xie, R., Ma, R., Li, D., Li, H., Guan, X., 2017. ACS Sens. 2, 703-709.

Rotem, D., Jayasinghe, L., Salichou, M., Bayley, H., 2012. J. Am. Chem. Soc. 134, 2781-2787.

Sadollahkhani, A., Hatamie, A., Nur, O., Willander, M., Zargar, B., Kazeminezhad, I., 2014. ACS Appl. Mater. Interfaces 6, 17694-17701.

Santos, C.I., Oliveira, E., Fernãndezlodeiro, J., Barata, J.F., Santos, S.M., Faustino, M.A., Cavaleiro, J.A., Neves, M.G., Lodeiro, C., 2013. Inorg. Chem. 52, 8564-8572.

Tian, K., Decker, K., Aksimentiev, A., Gu, L.Q., 2017. ACS Nano 11, 1204-1213.

Venkatesan, B.M., Bashir, R., 2011. Nat. Nanotechnol. 6, 615-624.

Wang, G., Wang, L., Han, Y., Zhou, S., Guan, X., 2014. Biosens. Bioelectron. 53, 453-458.

Wang, L., Yao, F., Kang, X.F., 2017. Anal. Chem. 89, 7958-7965.

Wang, Y., Yao, F., Kang, X.F., 2015. Anal. Chem. 87, 9991-9997.

Wen, S., Zeng, T., Liu, L., Zhao, K., Zhao, Y., Liu, X., Wu, H.-C., 2011. J. Am. Chem. Soc. 133, 18312-18317.

Xu, M., Gao, Z., Wei, Q., Chen, G., Tang, D., 2015. Biosens. Bioelectron. 74, 1-7.

Yang, C., Liu, L., Zeng, T., Yang, D., Yao, Z., Zhao, Y., Wu, H.-C., 2013. Anal. Chem. 85, 7302-7307.

Yin, B.C., Ye, B.C., Tan, W., Wang, H., Xie, C.C., 2009. J. Am. Chem. Soc. 131, 14624-14625.

Accepted manuscript

ACCEPTED MANUSCRIPT

Yusko, E.C., Prangkio, P., Sept, D., Rollings, R.C., Li, J., Mayer, M., 2012. ACS Nano 6, 5909-5919.

Zhang, X., Xu, X., Yang, Z., Burcke, A.J., Gates, K.S., Chen, S.J., Gu, L. Q., 2015. J. Am. Chem. Soc. 137, 15742-15752.

Accepted manuscript

ACCEPTED MANUSCRIPT

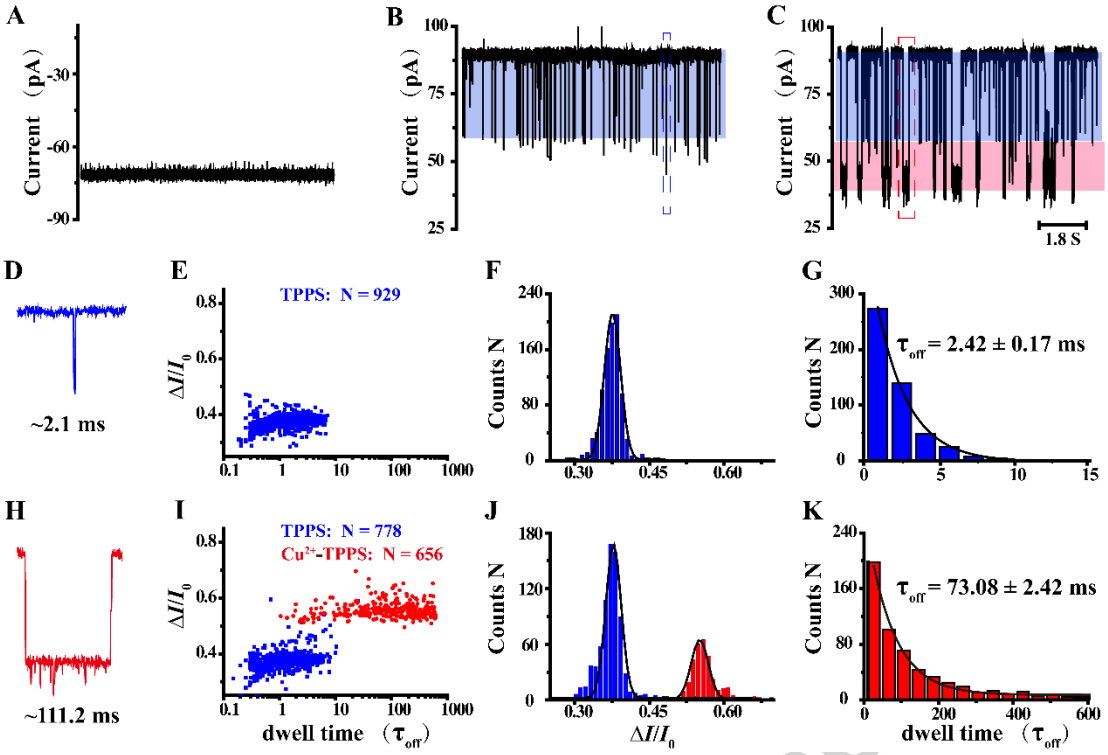

Fig. 1. Nanopore-based analysis of TPPS and Cu^{2+}-TPPS binding events. (A) No current modulation was observed with 5 μM TPPS in the trans chamber at the applied voltage of − 140 mV. (B) Representative single-channel current traces of TPPS interactions with the α-HL pore. (C) Representative single-channel current traces of TPPS after the addition of 10 μM Cu^{2+} to cis chamber. (D) Expanded view of a typical event indicated in the panel B. (E) Scatter plots the events caused by TPPS. (F) Histograms of normalized current blockade ($\Delta I/I_0$). (G) Histograms of dwell times of the TPPS. (H) Expanded view of a typical event indicated in the panel C. (I) Scatter plots the events caused by TPPS (blue) and Cu^{2+}-TPPS complexs (red). (J) Histograms of normalized current blockage ($\Delta I/I_0$). (K) Histograms of dwell times of the Cu^{2+}-TPPS. Experimental conditions: 1 M TMA-Cl and buffered with 10 mM NaAc/HAc (pH = 5.2), with transmembrane potential of + 140 mV.

Accepted manuscript

ACCEPTED MANUSCRIPT

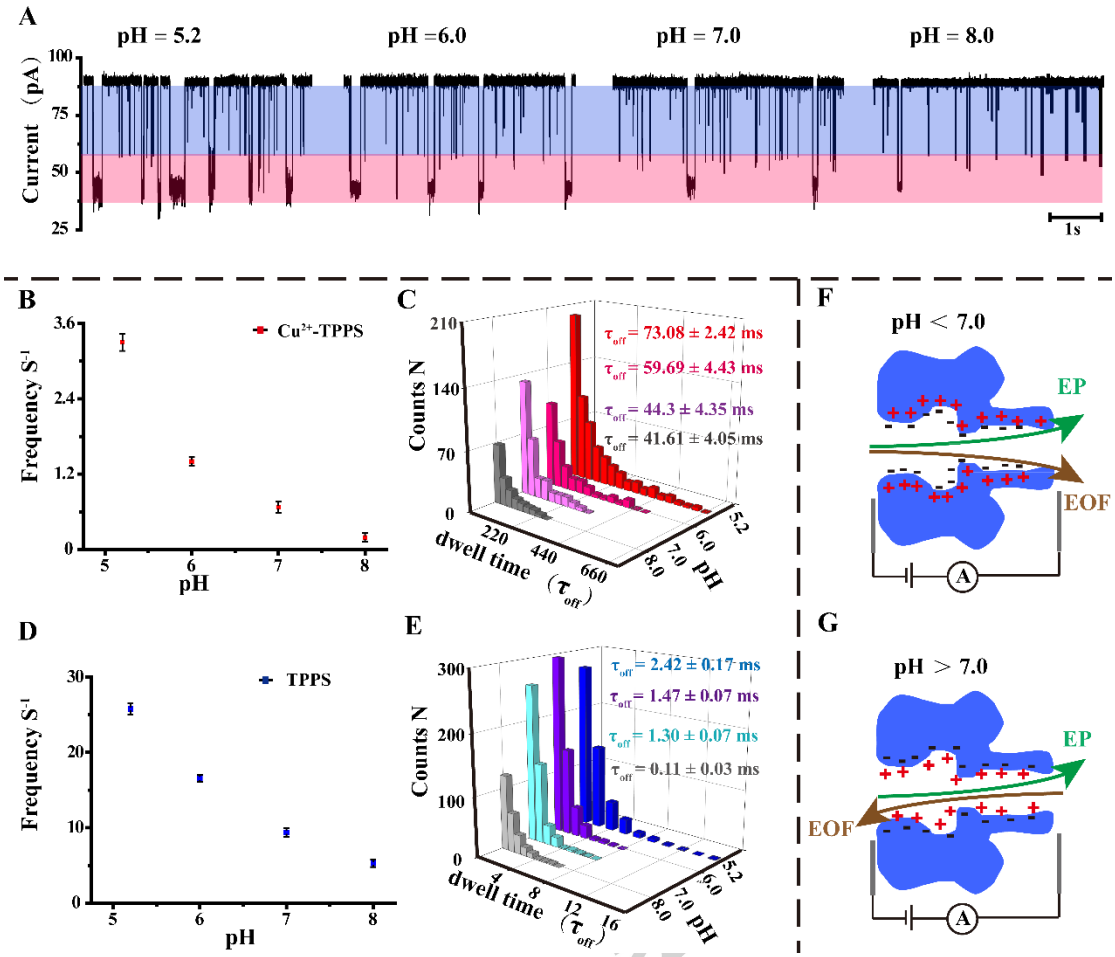

Fig. 2. (A) Typical single-channel current traces in different electrolyte pH, in the presence of 5 μM TPPS and 10 μM Cu^{2+} in the cis chamber. (B) The frequency of Cu^{2+}-TPPS complexes events at different electrolyte pH. (C) The dwell time of Cu^{2+}-TPPS complexes events at different electrolyte pH. (D) The frequency of TPPS in absence of Cu^{2+} at different electrolyte pH. (E) The dwell time of TPPS at different electrolyte pH. (F), (G) The combined action of EOF and EP on the interaction of negative charge analytes with α-HL nanopore at pH > 7.0 and pH < 7.0 respectively. Experimental conditions: 1 M TMA-Cl buffered with 10 mM NaAc/HAc (pH = 5.2, 6.0) or 10 mM PB (pH = 7.0 , 8.0), with transmembrane potential of + 140 mV.

Accepted Manuscript

ACCEPTED MANUSCRIPT

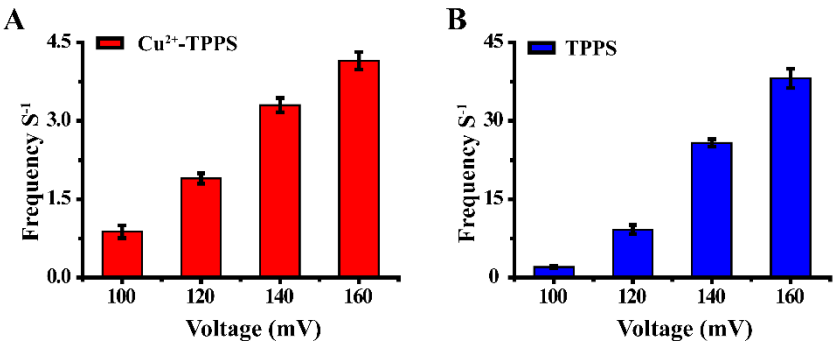

Fig. 3. (A) Effect of the applied potential bias on the Cu^{2+}-TPPS TPPS frequency in presence of 10 µM Cu^{2+}. (B) Effect of the applied potential bias on the TPPS frequency in absence of Cu^{2+}. Experimental conditions: 1 M TMA-Cl buffered with 10 mM NaAc/HAc (pH = 5.2), TPPS concentration was 5.0 µM.

Accepted manuscript

ACCEPTED MANUSCRIPT

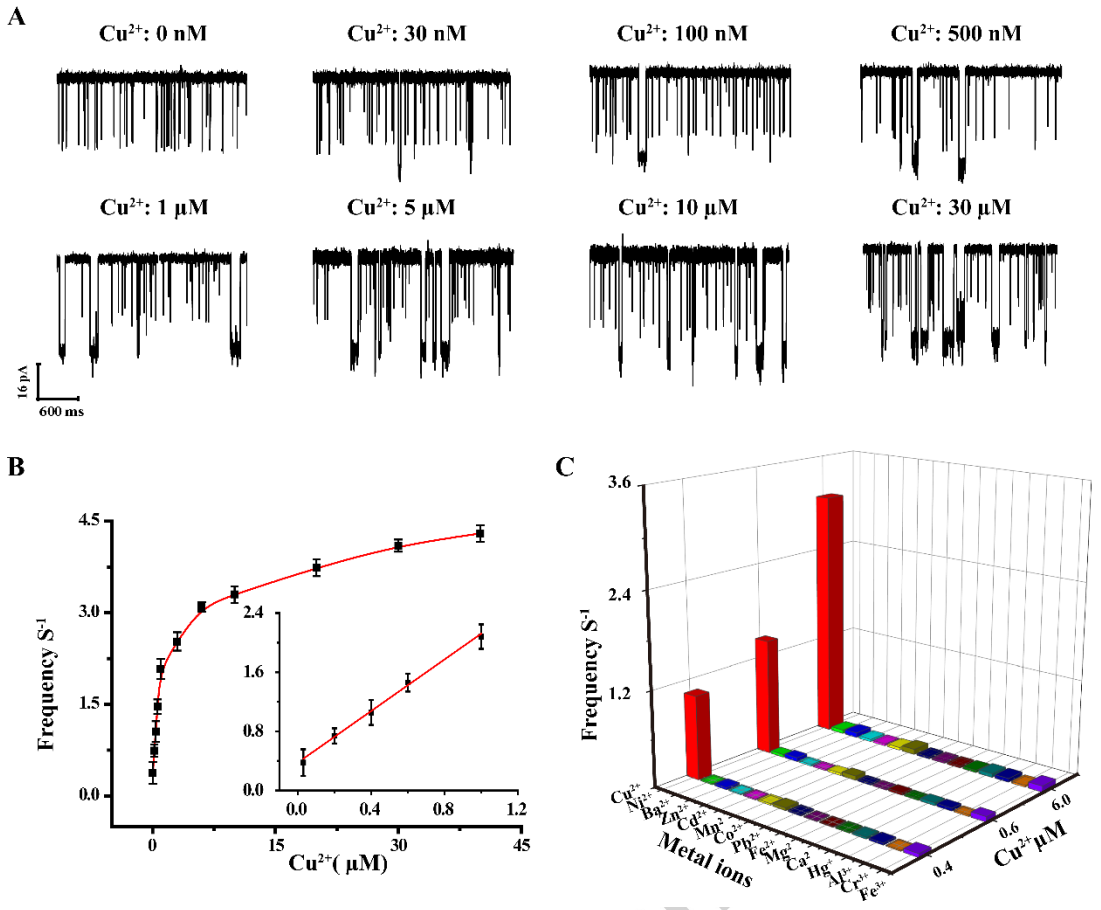

Fig. 4. Detection of Cu^{2+} at various concentrations. (A) Representative single-channel current traces showing various concentrations of copper ions added to the cis chamber in the presence of 5 μM TPPS probe. The concentration of copper ions were ranging from 0 nM to 30 μM, respectively (from up to down). (B) Dose-response curve for coppper ions nanopore sensor system. The inset of panel B shows an enlarged portion of the dose-response curve at a range 0.03-1.0 μM. (C) Selectivity for coppper ions nanopore sensor system. Experimental conditions: 1 M TMA-Cl buffered with 10 mM NaAc/HAc (pH = 5.2), with transmembrane potential of + 140 mV.

Accepted manuscript

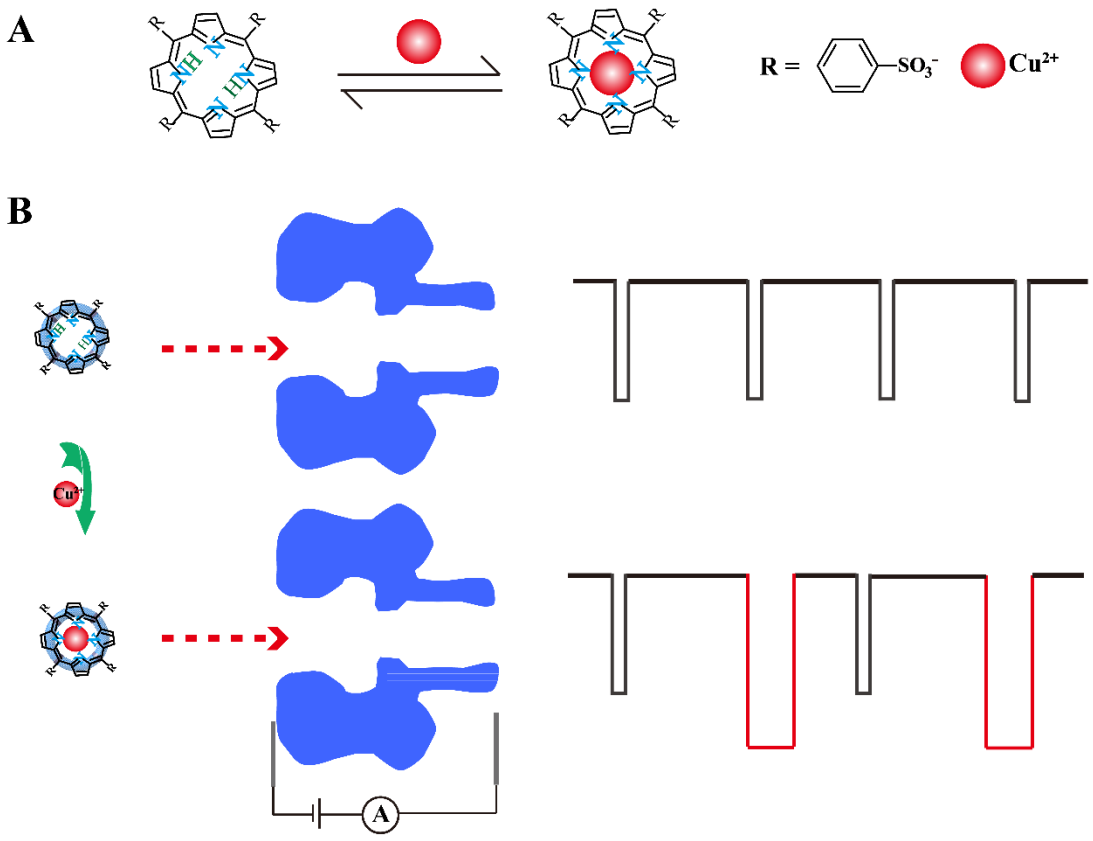

Scheme1. Nanopore detection of Cu^{2+} using a TPPS as probe. The TPPS and Cu^{2+}-TPPS complexes with the pore produced events having significantly different signatures, thus permitting them to be readily differentiated.

Table 1. Results of the detection of Cu^{2+} in real sample

Sample	Added Cu^{2+} (μM)	Measured (μM)	Recovery (100%)
Running water 1	0	0.12	—
Running water 2	0.2	0.31	95.0
Running water 3	0.4	0.51	97.5
Running water 4	0.6	0.73	101.7

Accepted manuscript

ACCEPTED MANUSCRIPT

Highlights

- We report a label-free nanopore sensing approach that enables investigation of metal ion-porphyrin interactions at single ion level.
- The unique nanopore sensor can provide a sensitive platform for detection of Cu^{2+} using TPPS as a recognition probe.
- The detection limit for Cu^{2+} is as low as 16 nM in aqueous solution.
- The proposed method has high selectivity and sensitivity to Cu^{2+}
- The nanopore sensor showed a promising potential for the detection of Cu^{2+} in real sample.

Accepted manuscript